EFFICIENCY OF POLYAMIDE THIN-FILM NANOCOMPOSITE MEMBRANE CONTAINING ZnO NANOPARTICLES

J. EL GHOUL[a,b*], I. GHILOUFI[a,b], A. S. AL-HOBAIB[c], L. EL MIR[a,b]
[a]*Al Imam Mohammad Ibn Saud Islamic University (IMSIU), College of Sciences, Department of Physics, Riyadh 11623, Saudi Arabia*
[b]*Laboratory of Physics of Materials and Nanomaterials Applied at Environment (LaPhyMNE), Gabes University, Faculty of Sciences of Gabes, 6072, Tunisia*
[c]*Institute of Atomic Energy Research, King Abdulaziz City for Science And Technology (KACST), 11442 P.O. Box 6086 Riyadh, Saudi Arabia*

We report in this study the synthesis of mixed matrix reverse osmosis membranes by interfacial polymerization (IP) of thin film nanocomposite (TFNC) on porous polysulfone supports (PS). This paper investigates the synthesis of ZnO nanoparticles (NPs) using the sol-gel processing technique and NPs enhanced membranes and evaluates the performance of mixed matrix membranes. Aqueous m-phenyl diamine (MPD) and organic trimesoyl chloride (TMC)-NPs mixture solutions were used in the IP process. The reaction of MPD and TMC at the interface of PS substrates resulted in the formation of the thin film composite (TFC). NPs of ZnO with a size of about 25 nm were used for the fabrication of the TFNC membranes. The TFNC membranes were characterized and evaluated in comparison with a (TFC) membrane. Their performances were evaluated based on the water permeability and salt rejection. Experimental results indicated that the NPs improved membrane performance under optimal weight NPs. By changing the content of the filler, better hydrophilicity was obtained; the contact angle was decreased from 94° to 18°. Also, the permeate water flux was increased from 26 to 48 L/m2.h when the weight of NPs is 0.007g with the maintaining of high salt rejection of 99%.

(Received February 21, 2017; Accepted May 12, 2017)

Keywords: Nano-ZnO; Interfacial polymerization; Nanocomposite; Nanofiltration, Desalination

1. Introduction

The growing demand for fresh water and the remarkable water crisis have spurred enormous interest in energy efficient technologies to produce safe drinking water from the ocean. Membrane filtration based on reverse osmosis (RO) is one of the most promising ways to desalinate seawater or brackish water, and thin film composite (TFC) membranes, comprised of ultra-thin active layers upon porous supports, have been widely used for this application[1, 2].Due to their completely hydrophilic characteristic and their certain functionality to benefit membrane properties of fouling reduction, inorganic materials incorporation into the polymer matrix is being of great interest [3]. Therefore, extensive efforts are being devoted to incorporate inorganic nanoparticles into polymeric membrane. It was reported that inorganic materials could be incorporated into membranes by doping and coating technologies [4, 5]. However, the doping technology has the disadvantage that inorganic materials are buried in the polymer matrix and in turn rendered non-functional. On the other hand, the coating technology has the disadvantage of the instability of inorganic materials onto polymer surface, especially for those not subject to chemical bonds or physical restraints between the inorganic materials and membrane matrix. The concept for formation of mixed matrix reverse osmosis membranes, by interfacial polymerization

*Corresponding authors: ghoultn@yahoo.fr

of nanocomposite thin films on porous supports, has been reported [6]. The emergence of nano-technology in membrane materials science could offer an attractive alternative to polymeric materials [7].Titanium oxide nanoparticles have been incorporated into polyamide (PA) thin film membranes by applying an in situ interfacial polymerization procedure [8]. Polyethersulfone–TiO2 nanoparticle composite membranes made from casting solution consisting of various compositions of polymer solvents (DMF and EtOH) and TiO_2 additive showed significant improvement in fouling resistance [9]. Silica oxide nanoparticles have been incorporated into PA thin film membrane via in situ interfacial polymerization process [10]. Zeolite nano-particles have been used to prepare nanocomposite membrane where first zeolite nano-particles are synthesized via a template hydrothermal reaction followed by a series of complex processes involving template removal, carbonization, sodium exchange and calcination [11]. Zirconium oxide has been used as a bulk material in polyvinylidene fluoride membranes [12]. ZnO enhanced polyethersulfone membrane has been synthesized by diffusion induced phase inversion in N-methyl-pyrrolidone. It has reported that membrane materials embedded with ZnO nanoparticles have significantly improved membrane features. It showed lower flux decline and better permeability compared to neat polymeric membrane due to a higher hydrophilicity of the ZnO membranes. ZnO nanoparticles provide a remarkable improvement in the methylene blue rejection potential [13]. Aluminum oxide (Al_2O_3) nanoparticles were also incorporated into a membrane of polyvinylidene fluoride using dimethyl acetamide as solvent [14]. Same type of polymer was used to prepare a membrane by doping with anhydrous and hydrated aluminum oxide particles through in situ particle embedment and subsequent crystal growth under a hydrothermal environment [3].

The lower cost of ZnO and the increase of the surface-to volume ratio obtained when ZnO is used as particles in a nano-sized scale make this alternative a potential system that can meet the demand of an efficient and lower-cost device. ZnO is one of the most important multifunctional semiconductor materials and exceptionally important for application in photo-catalysis and anti-bacterial materials, due to its excellent optical, electrical, mechanical and chemical properties [15, 16].

Furthermore, another issue that can limit the application of nanoparticles is their toxicity since it is thought that nanoparticles may persist as small particles in aquatic systems and that their bioavailability could be significantly greater than that of larger particles. For ZnO nanoparticles, positive conclusions have been obtained [17-19]. The use of nanoparticulate ZnO does not produce an increase in toxicity since the size distribution and surface area are not related to toxicity. Franklin et al. compared the toxicity in algae of nanoparticulate ZnO, bulk ZnO and $ZnCl_2$ and observed that toxicity is attributable solely to dissolved zinc, this is, to simple solubility of the compounds since ZnO nanoparticles aggregate in freshwater systems forming flocs of even several microns with a saturation solubility similar to that of bulk ZnO [20]. Also, since ZnO nanoparticles will be embedded in a solid matrix (the membrane), a stable system can be developed, keeping their physical properties associated to their size and the chemical activity related to their availability in the membrane. Thus, the use of ZnO in the nano-size scale incorporated in membranes is a promising and novel system that may be the solution for the development of low-cost and fouling-prevention membrane technology.

The novelty of this paper is in the synthesis of ZnO enhanced membranes in view to significantly enhance the performance of nanofiltration technology in terms of permeation, rejection and fouling resistance. The eventual membrane structure was also studied in this work.

2. Experimental

2.1. Synthesis of ZnO nanoparticles

ZnO nanocrystals were prepared by the sol–gel method using 16 g of zinc acetate dehydrate as precursor in a 112 ml of methanol. After 15 min magnetic stirring, the solution was placed in an autoclave and dried under supercritical conditions of ethyl alcohol (EtOH). The powder obtained is then annealed in an oven for 2 h at 500 ° C in air.

2.2. Preparation of the nanocomposite membranes

The polyamide TFC membrane was produced by immersing PS-20 (polysulfone supports) in an aqueous solution of 2% MPD (1,3-Phenylendiamine, >99%) for 2 min (the excess MPD solution was removed by rubber roller) followed by immersing the membrane in 0.1% TMC (1,3,5-benzenetricarbonyl trichloride, >98%)/hexane (99%) solution for 1 min, then rinsed with 0.2% Na2CO3 after that washed with DI water, finally stored in refrigerator ≈ 4°C in DI water till use. The Nanocomposite membranes were made by dispersing 0.003-0.009 g of synthesized ZnO nanoparticles in the TMC/hexane solution by ultrasonication for 1h at room temperature.

2.3. Characterization

The crystalline phases of the obtained nanopowders were identified by X-ray diffraction (XRD) using a Bruker D5005 powder X-ray diffractometer. Transmission electron microscopy (TEM, JEM-200CX) were used to study the morphology and particle size of the phosphor powders. The specimens for TEM were prepared by putting the as-grown products in EtOH and immersing them in an ultrasonic bath for 15 min, then dropping a few drops of the resulting suspension containing the synthesized materials onto TEM grid. The morphology and microstructure of the as-synthesized nanocomposite membrane was examined by means of scanning electron microscope (SEM, FEI Nova-Nano SEM-600,Netherlands). The quantitative analysis of the membranes was performed by the mean of energy-dispersive X-ray spectroscope (EDX). In addition, atomic force microscopy was used to analyze the surface morphology and roughness of the prepared membranes. The AFM device was Nanosurf scanning probe-optical microscope (Bruker Corporation). Small squares of the prepared membranes (approximately 1 cm^2) were cut and glued on glass substrate. Contact angle analysis was performed using a Ramé-Hart Model 250 Standard Goniometer/Tensiometer with DROP image Advanced software (Ramé-Hart Instrument Co., Succasunna, NJ 07876 USA). A water droplet was placed on a dry flat homogeneous membrane surface and the contact angle between the water and membrane was measured until no further change was observed. The average contact angle for distilled water was determined in a series of 8 measurements for each of the different membrane surfaces.

The performance of the prepared membranes was analyzed through a cross-flow system(CF042SS316 Cell, Sterlitech Corp.). The valid membrane area in this system was 42 cm^2. The Feed temperature was 25oC with pH adjusted between 6-7. The filtration was carried out at the pressure of 225 psi and the stirring speed of 2000 ppm. All measurements of the water flux and salt rejection were measured after 30 min of water filtration experiments to ensure that had reached stability. The flux was calculated with Eq. (1) :

$$J = \frac{V_p}{A*t} \tag{1}$$

where J is the water flux (L/m^2h), V_p is the permeate volume (L), A is the membrane area (m^2) and t is the treatment time (h).

The salt rejection was measured with Eq. (2) :

$$R = \left(1 - \frac{C_p}{C_f}\right)*100 \tag{2}$$

where R is the rejection ratio, C_p and C_f were the salt concentrations of permeate and feed, respectively.

3. Results and discussion

3.1. Characterization of the synthesized ZnO nanoparticles

The prepared ZnO nanoparticles were characterized by XRD, MET and HRMET. Figure 1 shows typical XRD spectra of the ZnO nanoparticles aerogel after thermal treatment. We noticed the appearance of nine pronounced diffraction peaks at 2θ = 31.82°, 34.61°, 36.36°, 47.55°, 56.73°, 62.88°, 66.34°, 68.08° and 69.19° which can be attributed to the (100), (002), (101), (102) (110), (103), (200), (112) and (201) planes of ZnO, respectively [21, 22]. Due to the small size of the crystallites in the aerogel, the diffraction lines are broadened and are further found to depend on the Miller indices of the corresponding sets of crystal planes. For our samples, the (002) diffraction line is always narrower than the (101) line and the latter is narrower than the (100) line. This indicated an asymmetry in the crystallite shape. The average grain size can be calculated using the Debye-Sherrer equation [23]:

$$G = 0.9\lambda / B\cos\theta_B \quad (3)$$

where λ is the X-ray wavelength (1. 5418 Å), θ_B is the maximum of the Bragg diffraction peak and B is the linewidth at half maximum. After a correction for the instrumental broadening, the obtained average value of the crystallites is 25 nm.

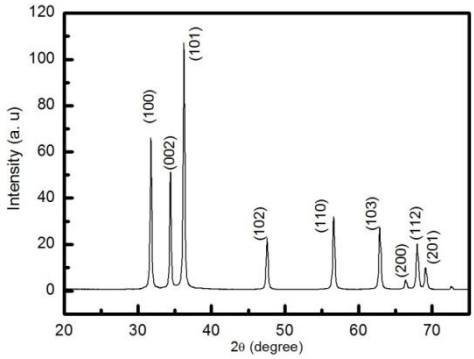

Fig.1. XRD patterns of nanoparticles ZnO (nano-ZnO)

Fig.2.a shows the TEM image for ZnO nanoparticles. It can be seen that the samples are nearly spherical with the diameters ranging from 18 to 30 nm, which is in agreement with XRD results. HRTEM image (Fig.2.b) showed that the measured distance between the planes is around 0.260 nm, which is corresponding to the (002) planes of the wurtzite ZnO.

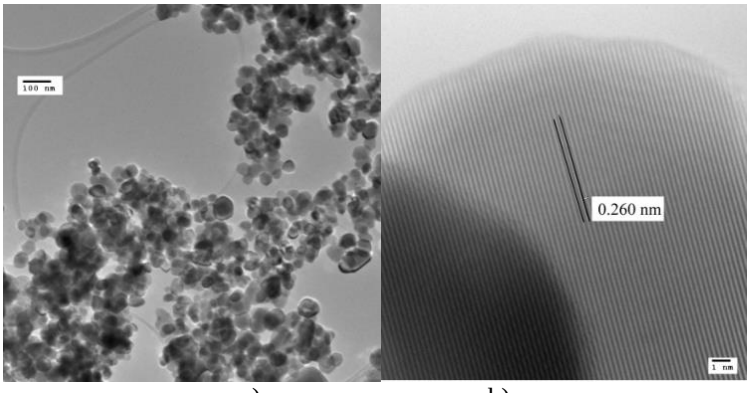

a) b)

Fig. 2. TEM image of nanoparticles ZnO (a) and HRTEM *of nanoparticles ZnO (b).*

3.2. Membranes characterizations

Membrane surfaces synthesized were observed with scanning electron microscopy (SEM)accompanied by EDX. Figure 3.a shows that the PS support layer was porous with a nanometric pore size, based on the calculation by the software Image J from a total of 1397 pore counts. After the IP process, the TFC membranes layer coated on the PS support layer by the reaction between MPD and TMC has led to a leaf-like morphology (Fig. 3.b).

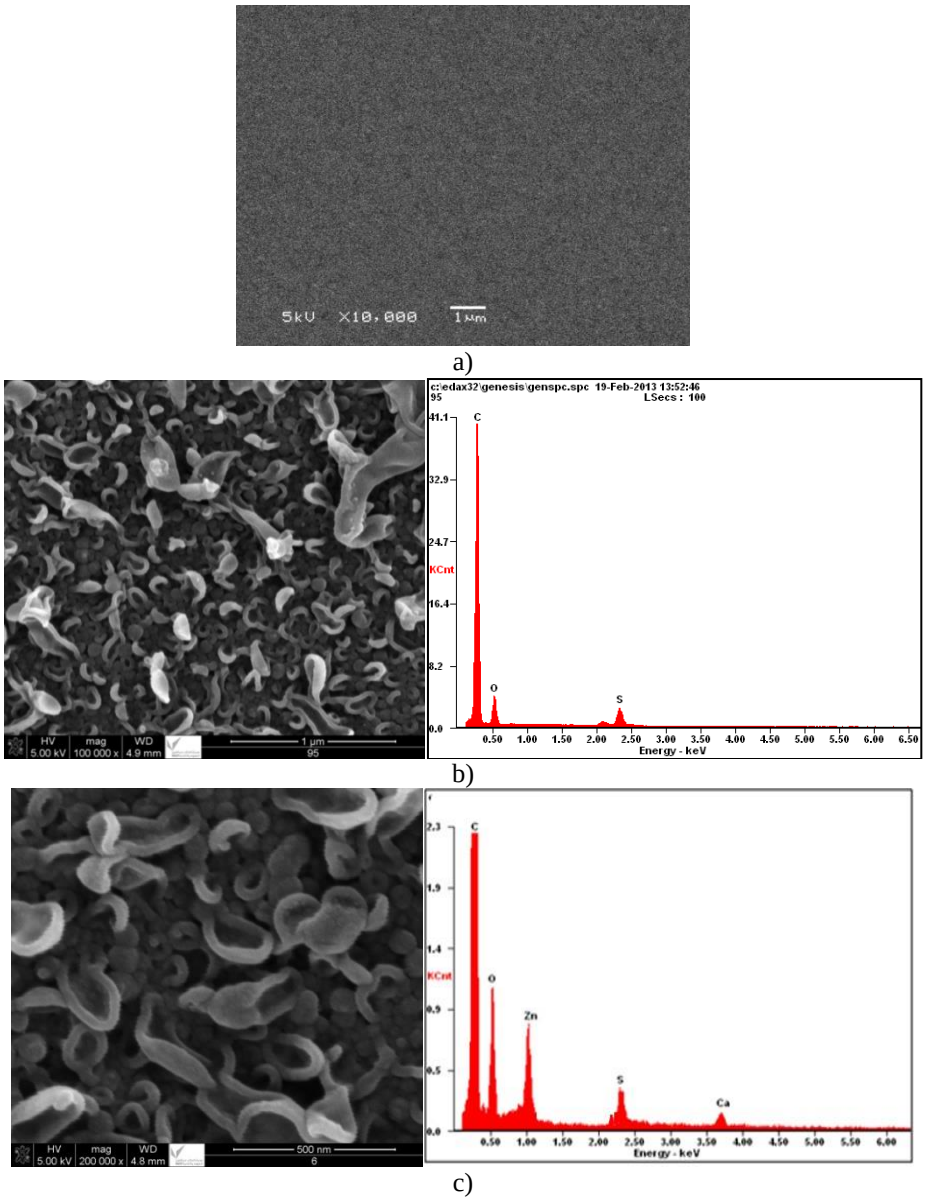

Fig. 3. SEM images and EDX analysis of membrane surface morphologies
(a) PS support layer; (b)TFC and (c) TFNC-0.007

The impregnation of ZnO-NPs does not have a great effect on the overall morphology of TFC in the tested weight range, but partial aggregation of ZnO-NPs was observed in samples (Fig. 3.c).

The difference between the images indicates clearly the presence of ZnO nanoparticles. This was further confirmed by EDX quantitative analysis which shows clearly the presence of carbon and oxygen with Zinc peaks as component elements.

AFM was used to further analyze the morphology of membrane surface. As shown in Fig.4 the TFC membrane showed much higher surface roughness (31 nm) due to the leaf-like shape of the PS support, consistent with the SEM observation (Fig. 3.a).The RMS value increased to 72 nm in the TFNC-0.007 membrane, which could be caused by the aggregation of ZnO-NPs on the membrane surface.

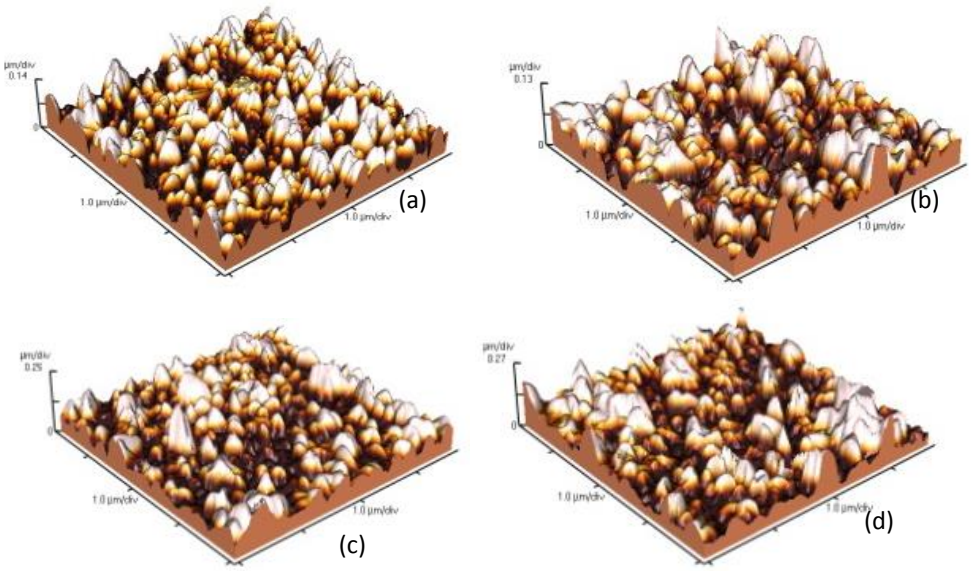

Fig. 4. AFM images of (a) TFC, (b) TFNC-0.003, (c) TFNC-0.005 and (d) TFNC-0.007 membrane

Our membranes were subjected to contact angle measurements. Standard deviations obtained on a single sample are of the order of a few degrees, which represent an acceptable reproducibility. Figure 5 shows measurements of the contact angle for the various weights of ZnO nanoparticles. The remarkable conclusion from Fig. 5 is that even at ultra-low weight (0.003 g), however, embedding ZnO nanoparticles into TFC membrane can drop contact angle significantly from 94° (control TFC membrane) to about 28°. In contrast, the hydrophilicity did not change significantly, in spite of the increasing content of ZnO nanoparticles. It is known that there is a strong correlation between the orientation (geometry) of water at a solid-liquid interface and the hydrophilicity of the solid surface [24]. The restructuring of interfacial water molecules can explain the increase of the hydrophilicity. The increased ordering of the interfacial water molecules improves the water molecule's ability to form hydrogen bonds and, in turn, produces stronger interactions between water and the solid phase (TFC surface).

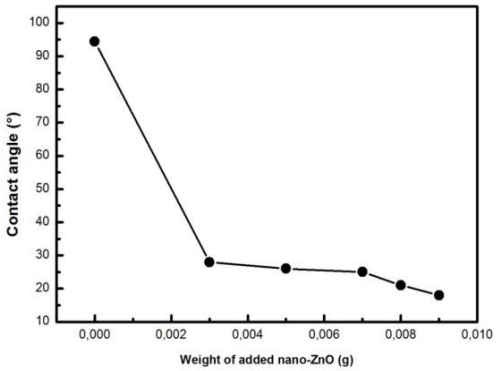

Fig. 5. Contact angle changes as the increasing weight of added nano-ZnO

The decrease of the contact angles in the presence of the embedded NPs could be caused by two reasons. First, the embedded spherical ZnO NPs can be exposed on the membrane surface. Therefore, the membrane surface hydrophilicity may increase because of the hydrophilic properties of these NPs. Embedding with ZnO NPs, the membrane surface could even become more hydrophilic due to the capability of the hydrophilic pores to imbibe water via capillary effects [25]. This is consistent with the result by Jeong et al. [6], who observed that the contact angle of membrane surface decreased with increasing Zeolite concentration and attributed this to the super-hydrophilic property of Zeolite. Second, the fact that NPs may hydrate and release heat when contacting with MPD aqueous solution [11]. This process may affect the IP reaction between MPD and TMC, and subsequently the chemical structure of the PS support. If more number of the acyl chloride groups in TMC remained on the surface without reaction with amine groups, the hydrolysis of acyl chloride could generate carboxylic acid functional groups; thus, surface hydrophilicity increased [26].Hydrophilic nano-ZnO significantly improves the hydrophilicity of the membranes. It is known that hydrophilicity is favorable for improving the water flux and antifouling ability.

It has been shown that the structure and hydrophilicity of the membrane are the two main factors that govern the filtration properties of membranes. The presence of hydrophilic nano-ZnO improves the hydrophilicity of membranes, which is much favorable to the water flux. Consequently, improved hydrophilicity and advantageous membrane structure contribute to higher water flux of hybrid membrane than that of TFC membrane[27]. The filtration properties of membranes have been obtained using the cross-flow system at 25 °C.

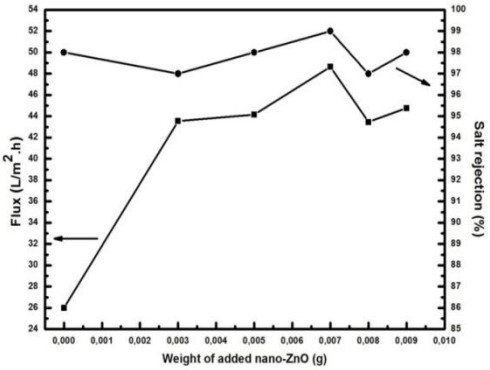

Fig. 6. Flux and rejection change as the increasing weight of added nano-ZnO

Fig.6 shows the water fluxes and the salt rejection of all the prepared membranes. The water fluxes of all the hybrid membranes are higher than that of the TFC membrane. As the weight of addednano-ZnO is increased, the water flux of the membrane increases to a peak value and then begins to decrease. The ZnO/TFC hybrid membrane exhibits the highest water flux (48.46 L/m^2h) when the concentration of added nano-ZnO is 0.007g. This flux represents an improvement of 191% over that of the TFC membrane. The salt rejection ratios of all the prepared membranes were unchanged. When the weight of added nano-ZnO exceeds 0.007g, the water flux begins to decrease. This phenomenon is the synergetic result of decreased porosity and aggregation of nano-ZnO.

4. Conclusions

ZnO nanoparticles (NPs) were synthesized, via sol–gel method, and characterized by X-ray diffractometer and Transmission electron microscope. The as synthesized NPs were embedded, with different weights, into polyamide membrane via interfacial polymerization process. The NPs strongly affects the properties of the membrane. SEM and EDX confirm the formation of polyamide membrane embedded with Zinc oxide nanoparticles. With increased weight of added

nano-ZnO, the contact angle continuously decreases. The contact angle of the membrane decreases from 94.4° to 28° when the weight of weight NPs is 0.003g.

The water flux of TFNC membrane is improved by the addition of NPs. The TFNC hybrid membrane exhibits the highest water flux (48.46 L/m^2h) when the weight of added NPs is 0.007g; this flux represents an improvement of 191% relative to that of the TFC membrane. In addition, the rejection of the TFNC membrane is not obviously changed.

Acknowledgements

The authors extend their appreciation to the Deanship of Academic Research at Al Imam Mohamed Ibn Saud Islamic University (IMSIU), Riyadh, Kingdom of Saudi Arabia, for funding the work through research project Number 361215, 1436H.

References

[1] R. J. Petersen, J. Membr. Sci.**83**,81 (1993).
[2] M. Wilf, The Guidebook of Membrane Desalination Technology, Balaban Desalination Publications, Italy (2007).
[3] A.S. AL-Hobaib, J. El Ghoul, I. Ghiloufi, L. El Mir, Materials Science in Semiconductor Processing **42,**111 (2016) .
[4]S.Y. Kwak,S.H. Kim, S.S. Kim, Env. Sci. Tech. **35**, 2388 (2001).
[5] D.J. Lin, C.L. Chang, F.M. Huang, L.P. Cheng, Polymer **44**, 413 (2003).
[6] B.H. Jeong, E.M.V. Hoek, Y. Yan, A.Subramani, X. Huang, G.Hurwitz, A.K.Ghosh, A.Jawor, J. Membr. Sci. **294**, 1 (2007).
[7] K.P. Lee, T.C.Arnot, D.Mattia, J. Membr. Sci. **370**, 1 (2011).
[8] S.H.S. Lee, J.Im, J.H.Kim, H.J.Kim, J.P.Kim, B.R.Min, Desalination **219**, 48 (2008).
[9] A. Sotto, A.Boromand, R.Zhang, P.Luis, J.M.Arsuaga, J.Kim, B.Van der Bruggen, J. Colloid Interf. Sci. **363**, 540 (2011).
[10] G.L. Jadav, P.S.Singh, J. Membr. Sci. **328**, 257 (2009).
[11] M.L. Lind, A.K.Ghosh, A.Jawor, X.Huang, W.Hou, Y.Yang, E.M.V.Hoek,Langmuir **25**, 10139 (2009).
[12] A. Bottino, G.Capannelli, A.Comite, Desalination **14**, 35 (2000).
[13] S. Balta, A.Sotto, P.Luis, I.Benea, B.Van der Bruggen, J.Kim, J. Membr. Sci. **389**, 155 (2012).
[14] L. Yan, Y.S. Li, C.B. Xiang,Polymer **46**, 7701 (2005).
[15] J. El Ghoul, N.Bouguila, S.A.Gómez-Lopera, L.El Mir, Superlattices and Microstructures **64**, 451 (2013).
[16]J. El Ghoul, J Mater Sci: Mater Electron **27**, 2159 (2016).
[17] J.H. Yuan, Y. Chen, H.X.Zha, L.J.Song, C.Y.Li, J.Q.Li, X.H.Xia, Colloids Surf. B **76**, 145 (2010).
[18] B. Berardis, G.Civitelli, M.Condello, P. Lista, R.Pozzi, G.Arancia, S.Meschini, Toxicol. Appl. Pharm. **246**, 116 (2010).
[19] W. Song, J.Zhang, J.Guo, J.Zhang, F.Ding, L.Li, Z.Sun, Toxicol. Lett. **199**, 389 (2010).
[20] N. Franklin, N.J.Rogers, S.C.Apte, G.E.Batley, G.E.Gadd, P.S.Casey, Environ. Sci. Technol. **41**, 8484 (2007).
[21]J. El Ghoul, Bull. Mater. Sci., **39**, 7 (2016).
[22]R. Krithiga, G.Chandrasekaran,Journal of Crystal Growth **311**, 4610 (2009).
[23] B. D. Cullity, Elements of X-ray Diffractions, Addison-Wesley, Reading, MA, 102 (1978).
[24] G. Hurwitz, G.R. Guillen, E.M.V. Hoek,J. Membr. Sci. **349**, 349 (2010).
[25] J. H. Li, Y.Y. Xu, L.P. Zhu, J. H.Wang, C. H.Du, J. Membr. Sci. **326**, 659 (2009).
[26] C. K. Kim, J.H.Kim, I.J.Roh, J.J.Kim, J. Membr. Sci. **165**, 189 (2000).
[27] H. Wu, B. Tang, P. Wu, J. Membr. Sci. **362**, 374 (2010).